



**HAL**  
open science

## How does the partition of unity influence SORAS preconditioner?

Marcella Bonazzoli, Xavier Claeys, Frédéric Nataf, Pierre-Henri Tournier

### ► To cite this version:

Marcella Bonazzoli, Xavier Claeys, Frédéric Nataf, Pierre-Henri Tournier. How does the partition of unity influence SORAS preconditioner?. 2022. hal-03882577v1

**HAL Id: hal-03882577**

**<https://hal.science/hal-03882577v1>**

Preprint submitted on 2 Dec 2022 (v1), last revised 18 Apr 2023 (v2)

**HAL** is a multi-disciplinary open access archive for the deposit and dissemination of scientific research documents, whether they are published or not. The documents may come from teaching and research institutions in France or abroad, or from public or private research centers.

L'archive ouverte pluridisciplinaire **HAL**, est destinée au dépôt et à la diffusion de documents scientifiques de niveau recherche, publiés ou non, émanant des établissements d'enseignement et de recherche français ou étrangers, des laboratoires publics ou privés.

# How does the partition of unity influence SORAS preconditioner?

Marcella Bonazzoli, Xavier Claeys, Frédéric Nataf and Pierre-Henri Tournier

## 1 Introduction

The Symmetrized Optimized Restricted Additive Schwarz (SORAS) preconditioner, first introduced in [8] for the Helmholtz equation and called OBDD-H, was later studied in [6] for generic symmetric positive definite problems and viewed as a symmetric variant of ORAS preconditioner. Its convergence was rigorously analyzed in [5] for the Helmholtz equation, and in [1] we generalized this theory to generic non self-adjoint or indefinite problems. Moreover, as an illustration of our theory, we proved new estimates for the specific case of the heterogeneous reaction-convection-diffusion equation. In the numerical experiments in [1], we noticed that the number of iterations for convergence of preconditioned GMRES appears not to vary significantly when increasing the overlap width. In the present paper, we show that actually this is due to the particular choice of the partition of unity for the preconditioner. The influence of five different kinds of partition of unity on SORAS solver and preconditioner for the Laplace equation has been briefly studied in the conclusion of [4], where the method is named ORASH. Here, for the reaction-convection-diffusion equation, we focus on two kinds for the partition of unity, and study the dependence on the overlap and on the number of subdomains.

---

Marcella Bonazzoli

Inria, UMA, ENSTA Paris, Institut Polytechnique de Paris, Palaiseau, France, e-mail: marcella.bonazzoli@inria.fr

Xavier Claeys

Sorbonne Université, CNRS, Université Paris Cité, LJLL, Paris, France, e-mail: xavier.claeys@sorbonne-universite.fr,

Frédéric Nataf

Sorbonne Université, CNRS, Université Paris Cité, Inria, LJLL, Paris, France, e-mail: frederic.nataf@sorbonne-universite.fr,

Pierre-Henri Tournier

Sorbonne Université, CNRS, Université Paris Cité, Inria, LJLL, Paris, France, e-mail: pierre-henri.tournier@sorbonne-universite.fr

## 2 SORAS preconditioner and two kinds of partition of unity

Let  $A$  denote the  $n \times n$  matrix, not necessarily positive definite nor self-adjoint, arising from the discretization of the problem to be solved, posed in an open domain  $\Omega \subset \mathbb{R}^d$ . Given a set of overlapping open subdomains  $\Omega_j, j = 1, \dots, N$ , such that  $\Omega = \cup_{j=1}^N \Omega_j$  and each  $\overline{\Omega_j}$  is a union of elements of the mesh  $\mathcal{T}^h$  of  $\Omega$ , we consider the set  $\mathcal{N}$  of the unknowns on the whole domain, so  $\#\mathcal{N} = n$ , and its decomposition  $\mathcal{N} = \cup_{j=1}^N \mathcal{N}_j$  into the non-disjoint subsets corresponding to the different overlapping subdomains  $\Omega_j$ , with  $\#\mathcal{N}_j = n_j$ . Denote by  $\delta$  the width of the overlap between subdomains. The following matrices are then the classical ingredients to define overlapping Schwarz domain decomposition preconditioners (see e.g. [2, §1.3]):

- restriction matrices  $R_j$  from  $\Omega$  to  $\Omega_j$ , which are  $n_j \times n$  Boolean matrices whose  $(i, i')$  entry equals 1 if the  $i$ -th unknown in  $\mathcal{N}_j$  is the  $i'$ -th one in  $\mathcal{N}$  and vanishes otherwise;
- extension by zero matrices  $R_j^T$  from  $\Omega_j$  to  $\Omega$ ;
- partition of unity matrices  $D_j$ , which are  $n_j \times n_j$  diagonal matrices with real non-negative entries such that  $\sum_{j=1}^N R_j^T D_j R_j = I$  and which can be seen as matrices that properly weight the unknowns belonging to the overlap between subdomains;
- local matrices  $B_j$ , of size  $n_j \times n_j$ , which arise from the discretization of sub-problems posed in  $\Omega_j$ , with for instance Robin-type or more general absorbing transmission conditions on the interfaces  $\partial\Omega_j \setminus \partial\Omega$ .

Then the one-level Symmetrized Optimized Restricted Additive Schwarz (SORAS) preconditioner is defined as

$$M^{-1} := \sum_{j=1}^N R_j^T D_j B_j^{-1} D_j R_j. \quad (1)$$

Note that  $M^{-1}$  is not self-adjoint when  $B_j$  is not self-adjoint, even if we maintain the SORAS name, where S stands for ‘Symmetrized’. In fact, this denomination was introduced in [6] for symmetric positive definite problems, since in that case SORAS preconditioner is a symmetric variant of ORAS preconditioner  $\sum_{j=1}^N R_j^T D_j B_j^{-1} R_j$ . Thus, the adjective ‘Symmetrized’ stands for the presence of the rightmost partition of unity  $D_j$ . We recall that ‘Restricted’ indicates the presence of the leftmost partition of unity  $D_j$  and that ‘Optimized’ refers to the choice of transmission conditions other than standard Dirichlet conditions in the local matrices  $B_j$ .

Here we focus on the influence exerted by the choice of partition of unity matrices  $D_j$  on the convergence of GMRES preconditioned by (1). Indeed, several definitions of the diagonal matrices  $D_j$  are possible to ensure property  $\sum_{j=1}^N R_j^T D_j R_j = I$ . In general, the diagonals of the  $D_j$  can be constructed by the interpolation of continuous partition of unity functions  $\chi_j: \Omega \rightarrow [0, 1], j = 1, \dots, N: \sum_{j=1}^N \chi_j = 1$  in  $\overline{\Omega}$ , and  $\text{supp}(\chi_j) \subset \Omega_j$ , so in particular  $\chi_j$  is zero on the subdomain interfaces  $\partial\Omega_j \setminus \partial\Omega$ .

In addition, in the case of ORAS fixed-point iterative solver, also the first derivatives of  $\chi_j$  are required to be equal to zero on  $\partial\Omega_j \setminus \partial\Omega$ , because this property ensures that the continuous version of ORAS solver is equivalent to Lions' algorithm, see e.g. [2, §2.3.2] for a particular model problem. An instructive calculation for a simple one- (and two-) dimensional problem, which shows an analogous equivalence property for RAS solver, is given in [3]; a more general equivalence result for ORAS solver is proved in [10, Theorem 3.4]. This first choice of Partition of Unity (PU1),

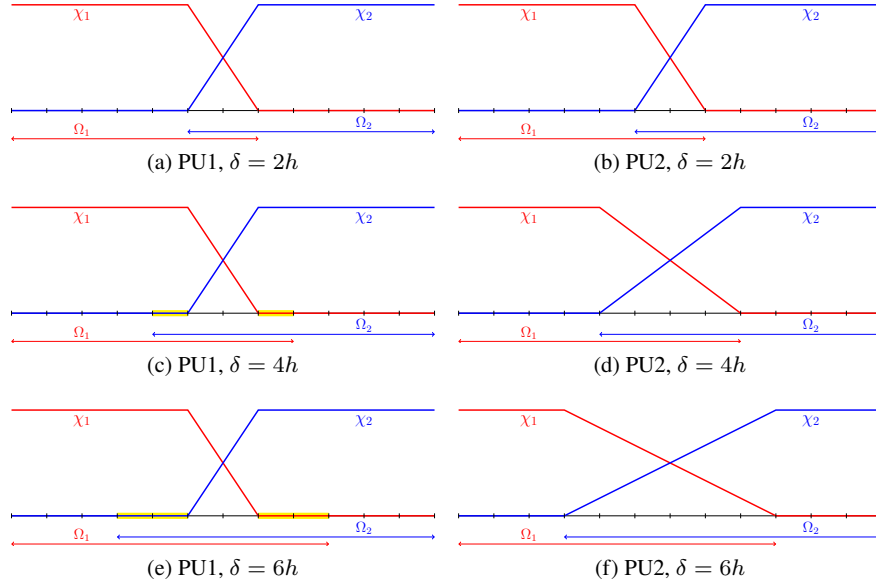


Fig. 1: Illustration in a one-dimensional two-subdomain case of the two kinds of partition of unity functions  $\chi_j : \Omega \rightarrow [0, 1]$  (PU1 on the left and PU2 on the right), with increasing width of the overlap  $\delta$  from top to bottom.

where the gradient of  $\chi_j$  is zero on the subdomain interfaces  $\partial\Omega_j \setminus \partial\Omega$ , is illustrated in a one-dimensional two-subdomain case in Figure 1, left, and starting from an overlap  $\delta = 4h$ . Note that PU1 in Figure 1 is actually different from the original RAS/ORAS partition of unity, which is defined for any overlap size  $\delta$  multiple of  $h$ , but essentially just at the discrete level, and takes only the values 0 or 1; in the original RAS/ORAS articles, the  $D_j$  are indeed hidden inside the definition of special extension matrices  $\tilde{R}_j^T$  related to an auxiliary non-overlapping partition of the domain (see e.g. [3, 10] and references therein). However, since the PU1 functions  $\chi_j$  in Figure 1 are symmetrical to each other, defining the  $D_j$  by interpolation of the  $\chi_j$  is more practical for a parallel implementation.

A second kind of Partition of Unity (PU2) is illustrated in Figure 1, right, where the  $\chi_j$  functions are different from zero in the interior of the whole overlapping region.

This choice is motivated by the fact that using PU1 for SORAS preconditioner can hinder the communication of information between subdomains since in (1) the matrix  $D_j$  is also applied before  $B_j^{-1}$ , that is before the local problem solve. Indeed, the numerical experiments performed in [1], where PU1 was used, show that the number of iterations for convergence of preconditioned GMRES does not vary significantly when increasing the overlap size (see also Tables 1,2,3 in Section 4).

### 3 Definition of the model problem

As in the second part of [1], we consider the heterogeneous reaction-convection-diffusion problem in conservative form, with Robin-type and Dirichlet boundary conditions:

$$\begin{cases} c_0 u + \operatorname{div}(\mathbf{a}u) - \operatorname{div}(\nu \nabla u) = f & \text{in } \Omega, \\ \nu \frac{\partial u}{\partial n} - \frac{1}{2} \mathbf{a} \cdot \mathbf{n} u + \alpha u = g & \text{on } \Gamma_R, \\ u = 0 & \text{on } \Gamma_D, \end{cases} \quad (2)$$

where  $\Omega \subset \mathbb{R}^d$  is an open bounded polyhedral domain,  $\partial\Omega = \Gamma = \Gamma_R \cup \Gamma_D$ ,  $\mathbf{n}$  is the outward-pointing unit normal vector to  $\Gamma$ ,  $c_0 \in L^\infty(\Omega)$ ,  $\mathbf{a} \in L^\infty(\Omega)^d$ ,  $\operatorname{div} \mathbf{a} \in L^\infty(\Omega)$ ,  $\nu \in L^\infty(\Omega)$ ,  $f \in L^2(\Omega)$ ,  $g \in L^2(\Gamma_R)$ ,  $\alpha \in L^\infty(\Omega)$  and all quantities are real-valued. We denote

$$\tilde{c} := c_0 + \frac{1}{2} \operatorname{div} \mathbf{a},$$

and suppose that there exist  $\tilde{c}_- > 0$ ,  $\tilde{c}_+ > 0$  such that

$$\tilde{c}_- \leq \tilde{c}(\mathbf{x}) \leq \tilde{c}_+ \text{ a.e. in } \Omega, \quad (3)$$

(which is a classical assumption in reaction-convection-diffusion equation literature), and that there exist  $\nu_- > 0$ ,  $\nu_+ > 0$  such that  $\nu_- \leq \nu(\mathbf{x}) \leq \nu_+$  a.e. in  $\Omega$ , and  $\alpha(\mathbf{x}) \geq 0$  a.e. in  $\Omega$ . Setting  $\mathbf{H}_{0,D}^1(\Omega) := \{v \in \mathbf{H}^1(\Omega) \mid v = 0 \text{ on } \Gamma_D\}$ , the variational formulation of problem (2) is (see e.g. [1, §4]): find  $u \in \mathbf{H}_{0,D}^1(\Omega)$  such that

$$a(u, v) = F(v), \quad \text{for all } v \in \mathbf{H}_{0,D}^1(\Omega), \quad (4)$$

where  $a$  is the following non-symmetric bilinear form

$$a(u, v) := \int_{\Omega} \left( \tilde{c}uv + \frac{1}{2} \mathbf{a} \cdot \nabla u v - \frac{1}{2} u \mathbf{a} \cdot \nabla v + \nu \nabla u \cdot \nabla v \right) + \int_{\Gamma_R} \alpha uv,$$

and

$$F(v) := \int_{\Omega} f v + \int_{\Gamma_R} g v.$$

On each subdomain  $\Omega_j$  we consider the local problem with bilinear form

$$a_j(u, v) := \int_{\Omega_j} \left( \tilde{c}uv + \frac{1}{2} \mathbf{a} \cdot \nabla u v - \frac{1}{2} u \mathbf{a} \cdot \nabla v + \nu \nabla u \cdot \nabla v \right) + \int_{\partial\Omega_j \setminus \Gamma_D} \alpha uv,$$

where we impose an absorbing transmission condition on the subdomain interface  $\partial\Omega_j \setminus \partial\Omega$  given by (see e.g. [7])

$$\alpha(\mathbf{x}) = \sqrt{(\mathbf{a} \cdot \mathbf{n})^2 + 4c_0\nu}/2.$$

## 4 Numerical experiments

Table 1: Iteration numbers for SORAS preconditioner with the two kinds of partition of unity, in the case of a convection field  $\mathbf{a} = 2\pi[-(y-0.1), (x-0.5)]^T$ , for different values of the overlap  $\delta$ , the reaction coefficient  $c_0$  and the viscosity  $\nu$ . The domain is decomposed into  $N = 5$  overlapping vertical strips and the global problem has 18361 degrees of freedom.

$\mathbf{a} = 2\pi[-(y-0.1), (x-0.5)]^T$	#PU1(PU2)			
	$\delta = 2h$	$\delta = 4h$	$\delta = 6h$	$\delta = 8h$
$c_0 = 1, \nu = 1$	21(21)	20(17)	20(15)	19(14)
$c_0 = 1, \nu = 0.001$	14(14)	13(11)	12(11)	12(10)
$c_0 = 0.001, \nu = 1$	21(21)	20(18)	20(15)	19(14)
$c_0 = 0.001, \nu = 0.001$	15(15)	14(12)	13(11)	13(11)

Table 2: Repeat of Table 1 but with  $\mathbf{a} = [-x, -y]^T$ . In this case  $\text{div } \mathbf{a} = -2$  is negative and  $\tilde{c} = c_0 - 1$  does not verify condition (3).

$\mathbf{a} = [-x, -y]^T$	#PU1(PU2)			
	$\delta = 2h$	$\delta = 4h$	$\delta = 6h$	$\delta = 8h$
$c_0 = 1, \nu = 1$	21(21)	21(19)	20(17)	20(15)
$c_0 = 1, \nu = 0.001$	16(16)	16(14)	16(13)	16(13)
$c_0 = 0.001, \nu = 1$	22(22)	22(19)	22(17)	21(16)
$c_0 = 0.001, \nu = 0.001$	17(17)	16(15)	16(14)	16(13)

We simulate problem (4) with  $\Omega$  a rectangle  $[0, N \cdot 0.2] \times [0, 0.2]$ , where  $N$  is the number of subdomains, and  $\Gamma_D = \Gamma$ ,  $\Gamma_R = \emptyset$ . In Tables 1,2,3 we take  $N = 5$  and

Table 3: Repeat of Table 1 but with  $\mathbf{a} = [1, 0]^T$  and with Streamline Upwind Petrov-Galerkin stabilization for the Galerkin approximation.

$\mathbf{a} = [1, 0]^T$	#PU1(PU2)			
	$\delta = 2h$	$\delta = 4h$	$\delta = 6h$	$\delta = 8h$
$c_0 = 1, \nu = 1$	20(20)	20(18)	20(16)	20(15)
$c_0 = 1, \nu = 0.001$	11(11)	11(12)	11(12)	11(12)
$c_0 = 0.001, \nu = 1$	20(20)	20(18)	20(16)	20(15)
$c_0 = 0.001, \nu = 0.001$	12(12)	12(12)	12(13)	12(12)

Table 4: Weak scaling test, with a regular decomposition into  $N$  vertical strips ( $\delta = 4h$ ). The global problem has 7381, 14701, 29341, 58621, 117181, 234301 degrees of freedom for  $N = 2, 4, 8, 16, 32, 64$  subdomains respectively.

$\mathbf{a} = [1, 0]^T$	#PU1(PU2)					
	$N = 2$	$N = 4$	$N = 8$	$N = 16$	$N = 32$	$N = 64$
$c_0 = 1, \nu = 1$	18(15)	23(20)	28(24)	35(28)	36(29)	36(29)
$c_0 = 1, \nu = 0.001$	8(8)	10(12)	16(16)	23(24)	37(37)	63(61)
$c_0 = 0.001, \nu = 1$	18(15)	23(20)	29(25)	35(29)	36(29)	36(29)
$c_0 = 0.001, \nu = 0.001$	8(8)	10(12)	16(17)	24(25)	40(40)	71(71)

Table 5: Weak scaling test as in Table 4, but with METIS decomposition into  $N$  arbitrary-shaped subdomains.

$\mathbf{a} = [1, 0]^T$	#PU1(PU2)					
	$N = 2$	$N = 4$	$N = 8$	$N = 16$	$N = 32$	$N = 64$
$c_0 = 1, \nu = 1$	21(18)	30(26)	40(33)	48(39)	53(41)	55(43)
$c_0 = 1, \nu = 0.001$	10(9)	12(12)	17(17)	25(24)	38(38)	63(62)
$c_0 = 0.001, \nu = 1$	21(18)	30(26)	40(33)	48(40)	54(42)	57(44)
$c_0 = 0.001, \nu = 0.001$	10(10)	12(12)	18(18)	26(26)	42(41)	73(72)

$f = 100 \exp \{-10((x - 0.5)^2 + (y - 0.1)^2)\}$ . In Tables 4, 5 we test weak scaling by varying  $N$ , with  $f = 100 \exp \{-10((x - 0.1)^2 + (y - 0.1)^2)\}$ . The problem is discretized by piece-wise linear Lagrange finite elements on a uniform triangular mesh with 60 points on the vertical side of the rectangle and  $N \cdot 60$  points on the horizontal one, resulting in 18361 degrees of freedom for  $N = 5$ , and 7381, 14701, 29341, 58621, 117181, 234301 degrees of freedom for  $N = 2, 4, 8, 16, 32, 64$  respectively. In Tables 1–4 the domain is partitioned into  $N$  vertical strips, while

in Table 5 it is partitioned into  $N$  arbitrary-shaped subdomains obtained using the automatic mesh partitioner METIS; then each subdomain is augmented with mesh elements layers of size  $\delta/2$  to obtain the overlapping decomposition: the total width of the overlap between two subdomains is then  $\delta$ . We use GMRES with right preconditioning, with a zero initial guess in Tables 1,2,3 and a random initial guess in Tables 4, 5. The stopping criterion is based on the relative residual, with a tolerance of  $10^{-6}$ . To apply the preconditioner, the local problems in each subdomain are solved with the direct solver MUMPS. All the computations are done in the `ffddm` framework [11] of FreeFEM.

We compare the number of iterations for convergence (denoted by # in the tables) using the two kinds of partition of unity: the results for PU1 were also included in [1] and the results for PU2 are reported inside brackets in Tables 1–5. In `ffddm` framework, the first partition of unity is selected by the flag `-raspart`, while the second partition of unity is the one used by default.

As in [1], we examine several configurations for the coefficients in (2). First, in Table 1 we consider a rotating convection field  $\mathbf{a} = 2\pi[-(y-0.1), (x-0.5)]^T$  and small/large values for the reaction coefficient  $c_0$  and the viscosity  $\nu$ . We can see that a larger overlap helps the convergence of the preconditioner, especially with PU2, while with PU1 the number of iterations does not vary significantly. Moreover, with both kinds of partition of unity, the number of iterations appears not very sensitive to the reaction coefficient  $c_0$ , while it increases when the viscosity  $\nu$  is larger.

Then, in Table 2 we take  $\mathbf{a} = [-x, -y]^T$ , which has negative divergence  $\operatorname{div} \mathbf{a} = -2$ , to test the robustness of the method when condition (3) on the positiveness of  $\tilde{c}$  is violated: in this case,  $\tilde{c} = c_0 - 1$ , so  $\tilde{c} = 0$ ,  $\tilde{c} = -0.999$  for  $c_0 = 1$ ,  $c_0 = 0.001$  respectively. We can still observe a convergence behavior similar to the one of Table 1.

Finally, in Table 3 we consider a horizontal convecting field  $\mathbf{a} = [1, 0]^T$ , which is normal to the interfaces between subdomains. Since in this case non-physical numerical instabilities appear in the solution, we stabilize the discrete variational formulation using the Streamline Upwind Petrov-Galerkin (SUPG) method, which adds to the Galerkin approximation the following term (see for instance [9, §11.8.6]):

$$\mathcal{L}_h(u_h, f; v_h) = \theta \sum_{\tau \in \mathcal{T}^h} \int_{\tau} (\mathcal{L}u_h - f) \frac{h_{\tau}}{|\mathbf{a}|} \mathcal{L}_{SS}v_h,$$

where  $\theta$  is a stabilization parameter (here we choose  $\theta = 0.15$ ),  $h_{\tau}$  is the diameter of the mesh element  $\tau$ , and

$$\mathcal{L}u_h = c_0 u_h + \operatorname{div}(\mathbf{a}u_h) - \operatorname{div}(\nu \nabla u_h), \quad \mathcal{L}_{SS}v_h = \frac{1}{2} \operatorname{div}(\mathbf{a}v_h) + \frac{1}{2} \mathbf{a} \cdot \nabla v_h.$$

In this configuration for the convecting field, for low viscosity  $\nu = 0.001$  the dependence of the iteration number on the overlap size  $\delta$  appears to be not significant, even with PU2.

To conclude, again in this third configuration with  $\mathbf{a} = [1, 0]^T$  and SUPG stabilization, we perform a weak scaling test by taking  $\Omega = [0, N \cdot 0.2] \times [0, 0.2]$  for



increasing number of subdomains  $N$ . First we consider a regular decomposition into vertical strips (Table 4) and then an arbitrary decomposition obtained by METIS (Table 5). In both tables, we fix the overlap  $\delta = 4h$ . Comparing Table 4 with Table 5, we can see that the number of iterations is higher when taking arbitrary-shaped subdomains. Moreover, especially in the cases with low viscosity  $\nu = 0.001$ , convergence deteriorates with  $N$ , as expected since we are testing a one-level preconditioner. In most tests, we can see that, for the considered SORAS preconditioner, using PU2 improves the iteration counts obtained with PU1.

In conclusion, our numerical investigation shows that, for the considered SORAS preconditioner, the second kind of partition of unity (PU2), which is non-zero in the interior of the whole overlapping region, generally improves the iteration counts obtained with the first kind of partition of unity (PU1), whose gradient is zero on the subdomain interfaces. Moreover, the first kind of partition of unity (PU1), which would be the natural choice for ORAS solver instead, yields for SORAS preconditioner iterations counts that do not vary significantly when increasing the overlap width.

## References

1. Bonazzoli, M., Claeys, X., Nataf, F., Tournier, P.H.: Analysis of the SORAS domain decomposition preconditioner for non-self-adjoint or indefinite problems. *Journal of Scientific Computing* **89**(1), 19 (2021). DOI 10.1007/s10915-021-01631-8
2. Dolean, V., Jolivet, P., Nataf, F.: An introduction to domain decomposition methods: algorithms, theory and parallel implementation. SIAM, Philadelphia, PA (2015). DOI 10.1137/1.9781611974065.ch1
3. Efstathiou, E., Gander, M.J.: Why Restricted Additive Schwarz converges faster than Additive Schwarz. *BIT Numerical Mathematics* **43**(5), 945–959 (2003). DOI 10.1023/B:BITN.0000014563.33622.1d
4. Gander, M.J.: Does the partition of unity influence the convergence of Schwarz methods? In: *Domain Decomposition Methods in Science and Engineering XXV*, pp. 3–15. Springer International Publishing, Cham (2020). DOI 10.1007/978-3-030-56750-7\_1
5. Graham, I.G., Spence, E.A., Zou, J.: Domain Decomposition with Local Impedance Conditions for the Helmholtz Equation with Absorption. *SIAM J. Numer. Anal.* **58**(5), 2515–2543 (2020). DOI 10.1137/19M1272512
6. Haferssas, R., Jolivet, P., Nataf, F.: A robust coarse space for optimized Schwarz methods: SORAS-GenEO-2. *C. R. Math. Acad. Sci. Paris* **353**(10), 959–963 (2015). DOI 10.1016/j.crma.2015.07.014
7. Japhet, C., Nataf, F., Rogier, F.: The optimized order 2 method: Application to convection–diffusion problems. *Future Generation Computer Systems* **18**(1), 17–30 (2001). DOI [https://doi.org/10.1016/S0167-739X\(00\)00072-8](https://doi.org/10.1016/S0167-739X(00)00072-8)
8. Kimm, J.H., Sarkis, M.: Restricted overlapping balancing domain decomposition methods and restricted coarse problems for the Helmholtz problem. *Comput. Methods Appl. Mech. Engrg.* **196**(8), 1507–1514 (2007). DOI 10.1016/j.cma.2006.03.016
9. Quarteroni, A.M.: *Numerical models for differential problems*, vol. 2. Springer (2009)
10. St-Cyr, A., Gander, M.J., Thomas, S.J.: Optimized Multiplicative, Additive, and Restricted Additive Schwarz preconditioning. *SIAM Journal on Scientific Computing* **29**(6), 2402–2425 (2007). DOI 10.1137/060652610
11. Tournier, P.H., Nataf, F.: FFDDM: FreeFEM Domain Decomposition Methods. <https://doc.freefem.org/documentation/ffddm/index.html> (2019)